

# Experimental Observation of Pentaatomic Tetracoordinate Planar Carbon-Containing Molecules

Lai-Sheng Wang,<sup>\*,†,‡</sup> Alexander I. Boldyrev,<sup>\*,§</sup> Xi Li,<sup>†,‡</sup> and Jack Simons<sup>\*,||</sup>

Contribution from the Department of Physics, Washington State University, Richland, Washington 99352, W. R. Wiley Environmental Molecular Sciences Laboratory, Pacific Northwest National Laboratory, MS K8-88, P.O. Box 999, Richland, Washington 99352, Department of Chemistry and Biochemistry, Utah State University, Logan, Utah 84322, and Department of Chemistry, University of Utah, Salt Lake City, Utah 84112

Received August 24, 1999

**Abstract:** The first neutral pentaatomic tetracoordinate planar carbon molecules,  $\text{CAI}_3\text{Si}$  and  $\text{CAI}_3\text{Ge}$ , as well as their anions,  $\text{CAI}_3\text{Si}^-$  and  $\text{CAI}_3\text{Ge}^-$ , were experimentally observed in the gas-phase and characterized by ab initio calculations and anion photoelectron spectroscopy. A four-center bond involving ligand–ligand interactions was found to be critical in stabilizing the planar structures of the 17-valence-electron  $\text{CAI}_3\text{Si}$  and  $\text{CAI}_3\text{Ge}$  and 18-valence-electron  $\text{CAI}_3\text{Si}^-$  and  $\text{CAI}_3\text{Ge}^-$ . These species violate the conventional expectation of tetrahedral structure for tetracoordinate carbon atoms and thus extend our concept of the range of chemical bonds that carbon can form.

## Introduction

That the tetracoordinate tetravalent carbon atom prefers a tetrahedral arrangement of its four ligands was first recognized independently by J. H. van't Hoff and J. A. LeBel in 1874. This contribution marks a milestone in understanding the structure and stereochemistry of carbon compounds. While the tetracoordinate tetrahedral carbon is firmly established in chemistry and elegantly explained by the concept of  $\text{sp}^3$ -hybridization, chemists have attempted for many years to make compounds containing *planar* tetracoordinate carbon. These efforts were reinforced by the pioneering theoretical formulation of hypothetical planar molecules by Hoffmann et al.<sup>1</sup> Schleyer and co-workers<sup>2–4</sup> have computationally tested and predicted a wide variety of candidate molecules for planar tetracoordinate carbon, many of which were reviewed recently.<sup>4</sup> Hoffmann et al.<sup>1</sup> initially considered the stabilization of planar-tetracoordinate carbon in fenestranes, in which a central carbon could potentially be locked in a nearly planar geometry due to steric constraints. Keese and co-workers<sup>5–7</sup> performed calculations on promising candidates and synthesized many such molecules. However, the most promising fenestrane molecule still has a bond angle of  $132.7^\circ$  at the central carbon.<sup>7</sup> Radom and co-workers<sup>8</sup> studied

computationally a class of polycyclic hydrocarbons, called alkapanes, in which a potential planar-tetracoordinate carbon can be achieved again by steric constraints. A divanadium complex, characterized structurally by Cotton and Miller,<sup>9</sup> is probably the first compound with a planar tetracoordinate carbon atom. A variety of organometallic compounds, mostly containing groups 4 and 5 elements, have since been reported by Erker, Gleiter, and co-workers<sup>10–12</sup> to possess planar tetracoordinate carbons.

Designing molecules with a planar tetracoordinate carbon atom requires overcoming carbon's inherent preference for tetrahedral bonding. There are two approaches, based on the previous investigations of many workers,<sup>1–12</sup> to achieving this goal. The electronic approach involves selecting substituents that preferentially stabilize a planar disposition of the carbon bonds over the normal tetrahedral arrangement. The alternative approach is based on using mechanical molecular strain forces exerted by the surrounding ligands to the carbon atom. This report deals with species for which the electronic effects are most important.

The difficulty of the task at hand can be appreciated by considering the kinds of bonds carbon can form in tetrahedral and in planar geometries, as first considered by Hoffmann et al.<sup>1</sup> In the former, the 2s and 2p valence orbitals are  $\text{sp}^3$ -hybridized to produce four  $\sigma$ -bonds to the four surrounding substituents. In the latter, the 2p valence orbital oriented perpendicular to the molecular plane is limited to forming a  $\pi$ -bond to the substituents; only the 2s and two of the 2p orbitals can form  $\sigma$ -bonds. Therefore, in the absence of any ligand–ligand interactions, tetrahedral bonding will be favored over planar bonding.

<sup>†</sup> Department of Physics, Washington State University.  
<sup>‡</sup> W. R. Wiley Environmental Molecular Sciences Laboratory, Pacific Northwest National Laboratory.  
<sup>§</sup> Department of Chemistry and Biochemistry, Utah State University.  
<sup>||</sup> Department of Chemistry, University of Utah.  
 (1) Hoffmann, R.; Alder, R. W.; Wilcox, C. F., Jr. *J. Am. Chem. Soc.* **1970**, *92*, 4992.  
 (2) Collins, J. B.; Dill, J. D.; Jemmis, E. D.; Apeloig, Y.; Schleyer, P. v. R.; Seeger, R.; Pople, J. A. *J. Am. Chem. Soc.* **1976**, *98*, 5419.  
 (3) Streitwieser, A.; Bachrach, S. M.; Dorigo, A.; Schleyer, P. v. R. *In Lithium Chemistry: A Theoretical and Experimental Overview*; Sapse, A.-M., Schleyer, P. v. R., Eds; Wiley: New York, 1995; p 1.  
 (4) Sorger, K.; Schleyer, P. v. R. *J. Mol. Struct.* **1995**, *338*, 317.  
 (5) Keese, R. *Nachr. Chem. Technol. Lab.* **1982**, *30*, 844.  
 (6) Agosta, W. C. Inverted and Planar Carbon. In *The Chemistry of Alkanes and Cycloalkanes*; Patai, S., Rappoport, Z., Eds.; Wiley, New York, 1992; Chapter 20.  
 (7) Luef, W.; Keese, R. *Adv. Strain Org. Chem.* **1993**, *3*, 229.

(8) (a) McGrath, M. P.; Radom, L. *J. Am. Chem. Soc.* **1992**, *114*, 8531.  
 (b) Rasmussen, D. R.; Radom, L. *Angew. Chem., Int. Ed.* **1999**, *38*, 2876.  
 (9) Cotton, F. A.; Millar, M. *J. Am. Chem. Soc.* **1977**, *99*, 7886.  
 (10) Erker, G. *Comments Inorg. Chem.* **1992**, *111*.  
 (11) Rottger D.; Erker, G. *Angew. Chem., Int. Ed. Engl.* **1997**, *36*, 812.  
 (12) Rottger, D.; Erker, G.; Fröhlich, R.; Grehl, M.; Silverio, S.; Hyla-Kryspin, I.; Gleiter, R. *J. Am. Chem. Soc.* **1995**, *117*, 10503.

Significant bonding among the four substituents must also be present to favor planar over tetrahedral geometries, as exemplified in a set of pentaatomic molecules ( $\text{CAI}_2\text{Si}_2$ ,  $\text{CGa}_2\text{Si}_2$ , and  $\text{CAI}_2\text{Ge}_2$ ) recently predicted to contain tetracoordinate planar carbon.<sup>13,14</sup> Essentially, the stability of the predicted planar tetracoordinate carbon can be related to the occurrence of 18-valence electrons because this number of electrons allows three  $\sigma$ -bonds and one  $\pi$ -bond to the central carbon atom (which alone will not be enough to render the planar structure more stable than the tetrahedral), four ligand-centered lone pairs, and, most importantly, one four-center ligand–ligand bond (the highest occupied molecular orbital, HOMO). However, there have been no experimental confirmations of these predictions or experimental observations of any such pentaatomic planar carbon molecules.

In the current work, we present the first experimental evidence of both neutrals and anions of pentaatomic tetracoordinate planar carbon molecules,  $\text{CAI}_3\text{Si}$  and  $\text{CAI}_3\text{Ge}$ , and  $\text{CAI}_3\text{Si}^-$  and  $\text{CAI}_3\text{Ge}^-$ , by a combined experimental and theoretical investigation. We created the anions in the gas phase using a laser vaporization cluster source and measured their photoelectron spectra. The theoretical calculations confirmed indeed that the 17-valence-electron systems ( $\text{CAI}_3\text{Si}$  and  $\text{CAI}_3\text{Ge}$ ) and the 18-valence-electron systems ( $\text{CAI}_3\text{Si}^-$  and  $\text{CAI}_3\text{Ge}^-$ ) are planar.

## Experimental Methods

The experiments were performed with a magnetic-bottle time-of-flight photoelectron spectroscopy (PES) apparatus equipped with a laser vaporization cluster source. Details of the experiment have been described previously.<sup>15</sup> Briefly,  $\text{CAI}_3\text{Si}^-$  and  $\text{CAI}_3\text{Ge}^-$  were produced by laser vaporization of a graphite/Al/Si and graphite/Al/Ge target, respectively, with a pure helium carrier gas. The clusters formed from the laser vaporization source were entrained in the He carrier gas and underwent a supersonic expansion. The anion species in the beam were extracted perpendicularly into a time-of-flight mass spectrometer. The anions of interest were selected and decelerated before photodetachment by a laser beam. For the current experiment, the fourth harmonic output (266 nm; 4.661 eV) from a Nd:YAG laser was used for the photodetachment PES experiments. The electron kinetic energy resolution of the apparatus was better than 30 meV for 1 eV electrons.

## Experimental Results

Figure 1 shows the mass spectra containing the species  $\text{CAI}_3\text{Si}^-$  and  $\text{CAI}_3\text{Ge}^-$  produced from the laser vaporization cluster source. Clusters with various compositions were observed. The  $\text{CAI}_3\text{Si}^-$  and  $\text{CAI}_3\text{Ge}^-$  species, focused in the current study, were produced quite abundantly with the  $\text{CAI}_3\text{Ge}^-$  peaks showing the correct isotope distributions (Figure 1b), mainly due to the natural isotopes of Ge. Figure 2 shows the photoelectron spectra of  $\text{CAI}_3\text{Si}^-$  and  $\text{CAI}_3\text{Ge}^-$ , measured at 4.661 eV photon energy. The two spectra are similar, with the  $\text{CAI}_3\text{Ge}^-$  spectrum slightly shifted to lower binding energies. Four major detachment features were observed in each and are labeled as X, A, B, and C. The vertical electron detachment energies of these features measured from the peak maxima are listed in Table 1 and are compared to ab initio calculations, as discussed below. Both spectra show a low-energy tail to peak X, which could be due to hot band transitions from vibrationally excited anions, geometry changes between the ground state of

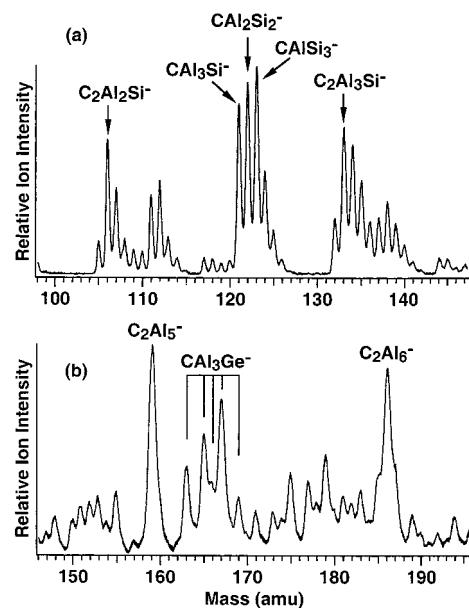


**Figure 1.** (a) Mass spectrum containing  $\text{CAI}_3\text{Si}^-$  and (b) mass spectrum containing  $\text{CAI}_3\text{Ge}^-$  with the five major natural isotopes of Ge labeled with the vertical lines.

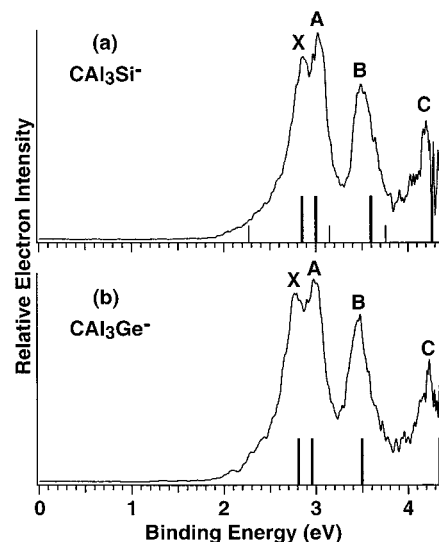


**Figure 2.** Photoelectron spectra of (a)  $\text{CAI}_3\text{Si}^-$  and (b)  $\text{CAI}_3\text{Ge}^-$  at 4.661 eV (266 nm). The thick and tall vertical bars mark the calculated vertical electron detachment energies for the tetracoordinate planar global minimum anions, and the thin and short vertical lines in (a) mark the calculated vertical electron detachment energies for the lowest-energy isomer (see text and Table 8).

the anion and the neutral, or isomers with lower electron binding energies. As we will show below, the latter is the major contributor to the tail.

## Computational Methods

In the theoretical investigation, we initially optimized a wide variety of structures of  $\text{CAI}_3\text{Si}$ ,  $\text{CAI}_3\text{Ge}$ ,  $\text{CAI}_3\text{Si}^-$ , and  $\text{CAI}_3\text{Ge}^-$ , employing analytical gradients with polarized split-valence basis sets ( $6\text{-}311+\text{G}^*$ ) using a hybrid method,<sup>16–18</sup> which includes a mixture of Hartree–Fock exchange with density functional exchange correlation known in the

(13) Schleyer P. v. R.; Boldyrev, A. I. *J. Chem. Soc., Chem. Commun.* **1991**, 1536.

(14) Boldyrev, A. I.; Simons, J. *J. Am. Chem. Soc.* **1998**, *120*, 7967.

(15) Wang, L. S.; Cheng, H. S.; Fan, J. *J. Chem. Phys.* **1995**, *102*, 9480. Wang L. S., Wu, H. In *Advances in Metal and Semiconductor Clusters. IV. Cluster Materials*; Duncan, M. A., Ed.; JAI Press: Greenwich, 1998; p 299.

(16) McLean, A. D.; Chandler, G. S. *J. Chem. Phys.* **1980**, *72*, 5639.

(17) Clark, T.; Chandrasekhar, J.; Spitznagel, G. W.; Schleyer, P. v. R. *J. Comput. Chem.* **1983**, *4*, 294.

(18) Frisch, M. J.; Pople, J. A.; Binkley, J. S. *J. Chem. Phys.* **1984**, *80*, 3265.

**Table 1.** Experimental and Theoretical Vertical Electron Detachment Energies (VDE) of  $\text{CAI}_3\text{Si}^-$  and  $\text{CAI}_3\text{Ge}^-$  and Theoretical Adiabatic Electron Detachment Energies (ADE)

	experimental VDE (eV)	electron detachment from MO <sup>a</sup>	theoretical <sup>b</sup> VDE (eV)	theoretical ADE (eV)
$\text{CAI}_3\text{Si}^-$				
X	2.88(5)	3b <sub>2</sub>	2.85 (0.87) <sup>c</sup>	2.67 <sup>d</sup>
A	3.03(4)	2b <sub>2</sub>	3.00 (0.87)	
B	3.49(3)	5a <sub>1</sub>	3.61 (0.86)	
C	4.20(4)	4a <sub>1</sub>	4.31 (0.84)	
$\text{CAI}_3\text{Ge}^-$				
X	2.78(4)	3b <sub>2</sub>	2.81 (0.87) <sup>e</sup>	2.66 <sup>d</sup>
A	2.98(4)	2b <sub>2</sub>	2.95 (0.87)	
B	3.47(3)	5a <sub>1</sub>	3.51 (0.86)	
C	4.23(4)	4a <sub>1</sub>	4.37 (0.84)	

<sup>a</sup> 3b<sub>2</sub> is the ligand–ligand bonding HOMO; the other three orbitals are ligand-centered nonbonding lone-pair orbitals. <sup>b</sup> At the OVGf/6-311+G(2df)//CCSD(T)/6-311+G\* level of theory. The pole strength is given in parentheses. <sup>c</sup> VDE = 2.86 eV at the CCSD(T)/6-311+G(2df)//CCSD(T)/6-311+G\* level of theory. <sup>d</sup> At the CCSD(T)/6-311+G(2df)//CCSD(T)/6-311+G\* level of theory. <sup>e</sup> VDE = 2.76 eV at the CCSD(T)/6-311+G(2df)//CCSD(T)/6-311+G\* level of theory.

literature as B3LYP.<sup>19–21</sup> Then, the geometries of the lowest-energy structures were refined at the second-order Møller–Plesset perturbation theory (MP2) level<sup>22</sup> and at the coupled cluster method (CCSD(T)) level of theory<sup>23–25</sup> using the same basis sets. Finally, the energies of the lowest-energy structures were refined using the CCSD(T) method and the more extended 6-311+G(2df) basis sets. Vertical electron detachment energies from the lowest-energy singlet structures of  $\text{CAI}_3\text{Si}^-$  and  $\text{CAI}_3\text{Ge}^-$  were calculated using the outer valence Green function (OVGF) method incorporated in Gaussian-94<sup>26–30</sup> and the 6-311+G(2df) basis sets. All core electrons were kept frozen in treating the electron correlation at the MP2 (except for the MP2 calculations of  $\text{CAI}_3\text{Si}$  and  $\text{CAI}_3\text{Si}^-$ , where all electrons were included in correlation), OVGF, and CCSD(T) levels of theory, and all calculations were performed using the Gaussian-94 program.<sup>31</sup>

## Theoretical Results

**$\text{CAI}_3\text{Si}^-$ .** We initially performed an exhaustive search for the global minimum of this anion at the B3LYP/6-311+G\* level of theory. More than 20 possible structures were tested in the

(19) Parr, R. G.; Yang, W. *Density-Functional Theory of Atoms and Molecules*; Oxford University Press: Oxford, 1989.

(20) Becke, A. D. *J. Chem. Phys.* **1992**, *96*, 2155.

(21) Perdew, J. P.; Chevary, J. A.; Vosko, S. H.; Jackson, K. A.; Pederson, M. R.; Singh, D. J.; Fiolhais, C. *Phys. Rev. B*, **1992**, *46*, 6671.

(22) Krishnan, R.; Binkley, J. S.; Seeger, R.; Pople, J. A. *J. Chem. Phys.* **1980**, *72*, 650.

(23) Cizek, J. *Adv. Chem. Phys.* **1969**, *14*, 35.

(24) Purvis, G. D., III; Bartlett, R. J. *J. Chem. Phys.* **1982**, *76*, 1910.

(25) Scuseria, G. E.; Janssen, C. L.; Schaefer, H. F., III. *J. Chem. Phys.* **1988**, *89*, 7282.

(26) Cederbaum, L. S. *J. Phys. B* **1975**, *8*, 290.

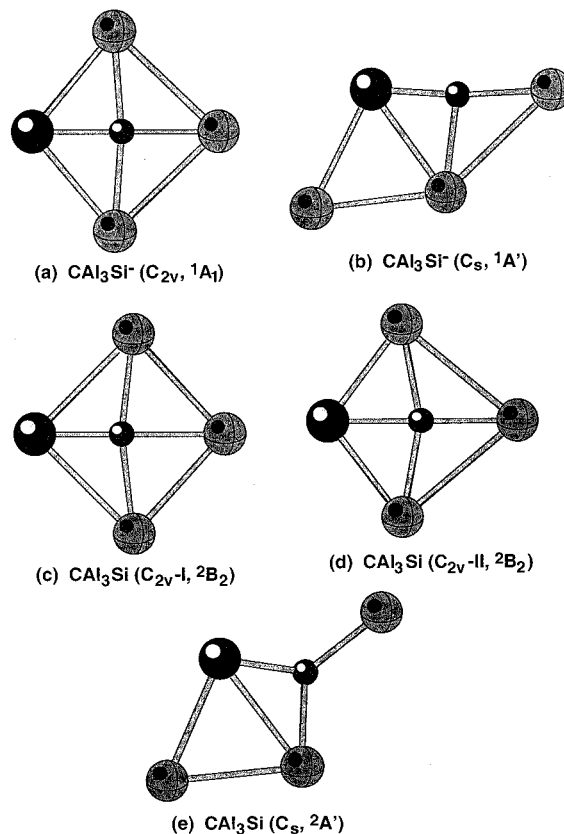
(27) von Niessen, W.; Shirmer J.; Cederbaum, L. S. *Comput. Phys. Rep.* **1984**, *1*, 57.

(28) Zakrzewski V. G.; von Niessen, W. *J. Comput. Chem.* **1993**, *14*, 13.

(29) Zakrzewski, V. G.; Ortiz, J. V. *Int. J. Quantum Chem.* **1995**, *53*, 583.

(30) Ortiz, J. V.; Zakrzewski, V. G.; Dolgunitcheva, O. In *Conceptual Trends in Quantum Chemistry*; E. S. Kryachko, E. S., Ed.; Kluwer; Dordrecht, 1997; Vol. 3, p 463.

(31) Frisch, M. J.; Trucks, G. W.; Schlegel, H. B.; Gill, P. M. W.; Johnson, B. G.; Robb, M. A.; Cheeseman, J. R.; Keith, T. A.; Peterson, G. A.; Montgomery, J. A.; Raghavachari, K.; Al-Laham, M. A.; Zakrzewski, V. G.; Ortiz, J. V.; Foresman, J. B.; Cioslowski, J.; Stefanov, B. B.; Nanayakkara, A.; Challacombe, M.; Peng, C. Y.; Ayala, P. Y.; Chen, W.; Wong, M. W.; Anders, J. L.; Replogle, E. S.; Gomperts, R.; Martin, R. L.; Fox, D. J.; Binkley, J. S.; DeFrees, D. J.; Baker, J.; Stewart, J. J. P.; Head-Gordon, M.; Gonzalez, C.; Pople J. A. *GAUSSIAN 94*, revision A.1; Gaussian Inc.: Pittsburgh, PA, 1995.

**Figure 3.** Optimized structures (at the B3LYP/6-311+G\* level of theory) of  $\text{CAI}_3\text{Si}^-$  and  $\text{CAI}_3\text{Si}$  (see Tables 2–5 for detailed parameters).**Table 2.** Calculated Molecular Properties of the  $\text{C}_{2v}$   $\text{CAI}_3\text{Si}^-$  Structure

	$\text{CAI}_3\text{Si}^- (\text{C}_{2v}, 1\text{A}_1)$		
	B3LYP/ 6-311+G*	MP2/ 6-311+G*	CCSD(T)/ 6-311+G*
$E_{\text{tot}}$ a.u.	−1055.008010	−1053.487833	−1053.021361
$R(\text{C}_1\text{—Si}_2)$ , Å	1.799	1.789	1.805
$R(\text{C}_1\text{—Al}_{3,4})$ , Å	2.028	2.013	2.018
$R(\text{C}_1\text{—Al}_5)$ , Å	1.962	1.970	1.961
$\angle\text{Si}_2\text{C}_1\text{Al}_{3,4}$ (deg)	86.2	87.5	86.2
$\nu_1$ (a <sub>1</sub> ), cm <sup>−1</sup>	929	987	
$\nu_2$ (a <sub>1</sub> ), cm <sup>−1</sup>	416	422	
$\nu_3$ (a <sub>1</sub> ), cm <sup>−1</sup>	303	326	
$\nu_4$ (a <sub>1</sub> ), cm <sup>−1</sup>	187	197	
$\nu_5$ (b <sub>1</sub> ), cm <sup>−1</sup>	178	81	
$\nu_6$ (b <sub>1</sub> ), cm <sup>−1</sup>	95	100i	
$\nu_7$ (b <sub>2</sub> ), cm <sup>−1</sup>	694	756	
$\nu_8$ (b <sub>2</sub> ), cm <sup>−1</sup>	269	283	
$\nu_9$ (b <sub>2</sub> ), cm <sup>−1</sup>	161	187	

singlet state. We also tested the triplet states corresponding to the few low-lying singlet structures. We found the lowest-energy structure to be the  $\text{C}_{2v}$  ( $1\text{A}_1$ ) planar structure (Figure 3a and Table 2). The next lowest-energy minimum of  $\text{CAI}_3\text{Si}^-$  corresponds to another planar  $\text{C}_{s,A}$  ( $1\text{A}'$ ) structure (Figure 3b and Table 4), which has a tricoordinate carbon and can be viewed as moving one corner-Al from the square-planar structure to one side of the square. This tricoordinate  $\text{C}_{s,A}$  isomer was found to be 22.5 kcal/mol higher in energy at the B3LYP/6-311+G\* level. We therefore concluded that the tetracoordinate  $\text{C}_{2v}$  ( $1\text{A}_1$ ) planar structure is the global minimum for the  $\text{CAI}_3\text{Si}^-$  anion at this level of theory.

When the more sophisticated MP2(full)/6-311+G\* level of theory was used,  $\text{CAI}_3\text{Si}^-$  was found to be slightly nonplanar (the deviation from planarity by carbon is less than 0.1 Å, Table



**Table 3.** Calculated Molecular Properties of the  $C_s$   $CAI_3Si^-$  and  $CAI_3Si$  Structures

	$CAI_3Si^- (C_s, ^1A')$		$CAI_3Si (C_s, I^2A'')$		$CAI_3Si (C_s, II^2A'')$
	MP2/6-311+G*	CCSD(T)/6-311+G*	MP2/6-311+G*	CCSD(T)/6-311+G*	MP2/6-311+G*
$E_{tot}$ , au	-1053.487878	-1053.021396	-1053.396126	-1052.932520	-1053.390735
$\Delta E_{tot}$ , kcal/mol <sup>a</sup>	-0.028	-0.022	-0.014	-0.006	-0.0025
$R(C_1-Si_2)$ , Å	1.791	1.805	1.745	1.754	1.909
$R(C_1-Al_{3,4})$ , Å	2.014	2.019	2.083	2.053	2.007
$R(C_1-Al_5)$ , Å	1.969	1.962	2.048	2.079	1.964
$\angle Si_2C_1Al_{3,4}$ (deg)	87.4	86.0	94.5	94.3	77.2
$\angle Si_2C_1Al_5$ (deg)	173.3	173.6	174.3	174.5	177.0
$\angle Al_5C_1Al_{3,4}$ (deg)	92.2	93.6	102.8	85.5	102.8
$\angle Al_3C_1Al_4$ (deg)	171.7	170.3	170.4	169.9	154.4
$\nu_1$ (a'), $cm^{-1}$	983		1091		828
$\nu_2$ (a'), $cm^{-1}$	424		378		420
$\nu_3$ (a'), $cm^{-1}$	325		255		277
$\nu_4$ (a'), $cm^{-1}$	197		161		211
$\nu_5$ (a'), $cm^{-1}$	122		119		147
$\nu_6$ (a'), $cm^{-1}$	98		66		43
$\nu_7$ (a''), $cm^{-1}$	753		803		729
$\nu_8$ (a''), $cm^{-1}$	284		296		279
$\nu_9$ (a''), $cm^{-1}$	188		201		50

<sup>a</sup> Relative to the corresponding planar structure.

3), but with bond lengths and valence angles being essentially the same as those obtained at the B3LYP/6-311+G\* level. Moreover, the energy difference between the perfectly planar structure and the slightly nonplanar global minimum structure (0.028 kcal/mol, Table 3) was smaller than the difference in the zero-point energies (ZPEs) (0.192 kcal/mol). Therefore, the vibrationally averaged structure of  $CAI_3Si^-$  is actually planar. Further test for planarity was made using CCSD(T)/6-311+G\* geometry optimizations (Table 3). For  $CAI_3Si^-$  we found the same deviation from planarity as at the MP2/6-311+G\* level of theory. The energy of planarization was found to be even smaller (0.022 kcal/mol, Table 3) at this level of theory.

The  $C_{s,A}$  ( $^1A'$ ) structure of  $CAI_3Si^-$  was also reoptimized at the MP2(full)/6-311+G\* level, and found to be planar at this level of theory. At our highest level of theory (CCSD(T)/6-311+G(2df)), the  $C_{s,A}$  ( $^1A'$ ) structure was found to be 24.5 kcal/mol higher than the global minimum.

**$CAI_3Si$ .** Initially, we performed a similarly exhaustive search for the global minimum of the neutral  $CAI_3Si$  at the B3LYP/6-311+G\* level of theory. We found two low-energy structures,  $C_{2v-I}$  ( $^2B_2$ ) and  $C_{2v-II}$  ( $^2B_2$ ) (Figure 3 and Table 4), which are closely related to the  $C_{2v}$  ( $^1A_1$ ) planar structure of the anion. The  $C_{2v-I}$  ( $^2B_2$ ) structure is more stable than the  $C_{2v-II}$  ( $^2B_2$ ) by 2.5 kcal/mol. At the MP2(full)/6-311+G\* level of theory, both the  $C_{2v-I}$  and  $C_{2v-II}$  structures of  $CAI_3Si$  were found to be slightly nonplanar (Table 5). Again, the energy differences between the perfectly planar structures and the slightly nonplanar global minimum structures (0.014 kcal/mol for  $C_{2v-I}$  and 0.0025 kcal/mol for  $C_{2v-II}$ ) were smaller than the corresponding differences in the ZPEs (0.225 kcal/mol for  $C_{2v-I}$  and 0.152 kcal/mol for  $C_{2v-II}$ ). Therefore, the vibrationally averaged structures of  $CAI_3Si$  remain planar. A further test for planarity was made using CCSD(T)/6-311+G\* geometry optimizations. At this level of theory, the  $C_{2v-II}$  ( $C_s-II$ ) structure collapsed into the  $C_{2v-I}$  ( $C_s-I$ ) structure upon geometry optimization. Therefore, at our highest level of theory we have only one  $C_{2v-I}$  ( $C_s-I$ ) structure (Table 3). We found the same deviations from planarity at the CCSD(T)/6-311+G\* level of theory as at MP2(full)/6-311+G\*. Again, when the ZPEs are taken into account, the vibrationally averaged structures of  $CAI_3Si$  remain planar.

The tricoordinate  $C_{s,A}$  isomer was found to be 7.8 kcal/mol higher in energy at the B3LYP/6-311+G\* level (Table 4) and 10.3 kcal/mol higher in energy at the CCSD(T)/6-311+G(2df)

**Table 4.** Calculated Molecular Properties of the Alternative Local Minimum  $C_{s,A}$   $CAI_3Si^-$ , and  $CAI_3Si$  Structures

	$CAI_3Si^- (C_{s,A} ^1A')$		$CAI_3Si (C_{s,A} ^2A')$
	B3LYP/6-311+G*	MP2(full)/6-311+G*	B3LYP/6-311+G*
$E_{tot}$ , au	-1054.972102	-1053.444589	-1054.903599
$\Delta E_{tot}$ , kcal/mol <sup>a</sup>	22.5	27.2	7.8
$R(C_1-Si_2)$ , Å	1.760	1.767	1.754
$R(C_1-Al_3)$ , Å	3.761	3.741	3.585
$R(C_1-Al_4)$ , Å	2.010	2.020	1.944
$R(C_1-Al_5)$ , Å	1.915	1.935	1.963
$\angle Si_2C_1Al_3$ (deg)	41.8	40.5	47.5
$\angle Al_3C_1Al_4$ (deg)	45.0	44.4	49.5
$\angle Al_4C_1Al_5$ (deg)	100.0	93.0	130.4
$\nu_1$ (a'), $cm^{-1}$	1022	1042	971
$\nu_2$ (a'), $cm^{-1}$	554	577	686
$\nu_3$ (a'), $cm^{-1}$	453	452	396
$\nu_4$ (a'), $cm^{-1}$	307	336	265
$\nu_5$ (a'), $cm^{-1}$	266	282	211
$\nu_6$ (a'), $cm^{-1}$	185	226	178
$\nu_7$ (a'), $cm^{-1}$	94	129	70
$\nu_8$ (a''), $cm^{-1}$	142	95	166
$\nu_9$ (a''), $cm^{-1}$	47	27	50

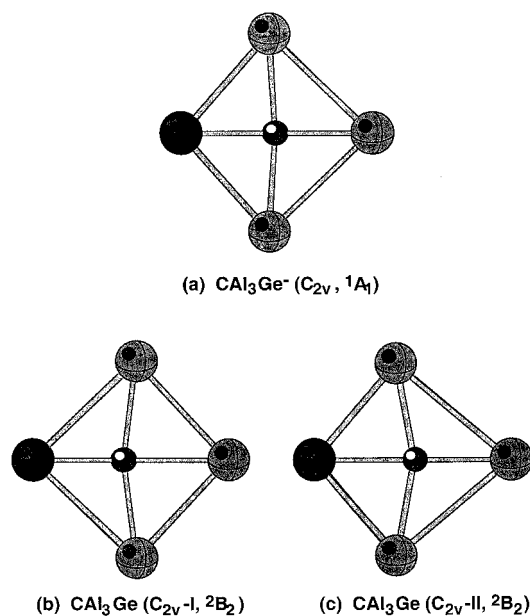
<sup>a</sup> Relative to the corresponding global minimum structure.

level of theory. We therefore concluded that the tetracoordinate  $C_{2v-I}$  ( $C_s-I$ ) planar structure is the global minimum for the  $CAI_3Si$  neutral molecule.

**$CAI_3Ge^-$ .** For  $CAI_3Ge^-$ , we assumed that it would have a similar global minimum as  $CAI_3Si^-$ , based on their nearly identical PES spectra (Figure 2). Hence we started our optimization with the  $C_{2v}$  ( $^1A_1$ ) planar structure (Figure 4 and Table 6) at the B3LYP/6-311+G\* level of theory. Indeed this structure was found to be a minimum. At the MP2/6-311+G\* level,  $CAI_3Ge^-$  was again found to be slightly nonplanar. The energy difference between the perfectly planar structure and the slightly nonplanar global minimum structure (0.0067 kcal/mol) was again smaller than the difference in the ZPEs (0.061 kcal/mol). Thus, the vibrationally averaged structure of  $CAI_3Ge^-$  remains planar. However, at our highest level of theory (CCSD(T)/6-311+G\*) we found a perfectly planar structure for  $CAI_3Ge^-$ , that is, when geometry optimization was performed within  $C_s$  symmetry it converged to the planar structure (Table 6). We further optimized the tricoordinate  $C_{s,A}$  isomer, which was

**Table 5.** Calculated Molecular Properties of the  $C_{2v}$   $CAI_3Si$  Structures

	$CAI_3Si$ ( $C_{2v}$ , $1^2B_2$ )			$CAI_3Si$ ( $C_{2v}$ , $II^2B_2$ )		
	B3LYP/6-311+G*	MP2/6-311+G*	CCSD(T)/6-311+G*	B3LYP/6-311+G*	MP2/6-311+G*	CCSD(T)/6-311+G*
$E_{tot}$ a.u.	-1054.915950	-1053.396103	-1052.932510	-1054.912044	-1053.390731	-1052.927941
$\Delta E_{tot}$ (kcal/mol)	0.0	0.0	0.0	2.45	3.37	2.87
$R(C_1-Si_2)$ , Å	1.745	1.745	1.754	1.891	1.907	1.890
$R(C_1-Al_{3,4})$ , Å	2.047	2.047	2.052	2.010	2.008	2.017
$R(C_1-Al_5)$ , Å	2.101	2.082	2.078	1.979	1.964	1.974
$\angle Si_2C_1Al_{3,4}$ (deg)	96.9	94.5	94.4	79.2	77.2	79.3
$\nu_1$ ( $a_1$ ), $cm^{-1}$	962	1091		829	830	
$\nu_2$ ( $a_1$ ), $cm^{-1}$	359	376		402	420	
$\nu_3$ ( $a_1$ ), $cm^{-1}$	237	256		281	277	
$\nu_4$ ( $a_1$ ), $cm^{-1}$	175	159		218	211	
$\nu_5$ ( $b_1$ ), $cm^{-1}$	178	65		205	123	
$\nu_6$ ( $b_1$ ), $cm^{-1}$	74	42i		78	61i	
$\nu_7$ ( $b_2$ ), $cm^{-1}$	540	783		627	690	
$\nu_8$ ( $b_2$ ), $cm^{-1}$	235	276		315	233	
$\nu_9$ ( $b_2$ ), $cm^{-1}$	59	205		71	94	

**Figure 4.** Optimized structures (at the B3LYP/6-311+G\* level of theory) of  $CAI_3Ge^-$  and  $CAI_3Ge$  (see Tables 6 and 7 for detailed parameters).**Table 6.** Calculated Molecular Properties of the  $C_{2v}$   $CAI_3Ge^-$  Structure

	$CAI_3Ge^-$ ( $C_{2v}$ , $1A_1$ )		
	B3LYP/6-311+G*	MP2/6-311+G*	CCSD(T)/6-311+G*
$E_{tot}$ , au	-2842.522885	-2839.373522	-2839.426811
$R(C_1-Ge_2)$ , Å	1.908	1.900	1.919
$R(C_1-Al_{3,4})$ , Å	2.021	2.018	2.018
$R(C_1-Al_5)$ , Å	1.965	1.977	1.965
$\angle Ge_2C_1Al_{3,4}$ (deg)	86.5	88.3	86.9
$\nu_1$ ( $a_1$ ), $cm^{-1}$	826	872	
$\nu_2$ ( $a_1$ ), $cm^{-1}$	354	359	
$\nu_3$ ( $a_1$ ), $cm^{-1}$	281	298	
$\nu_4$ ( $a_1$ ), $cm^{-1}$	174	179	
$\nu_5$ ( $b_1$ ), $cm^{-1}$	182	84	
$\nu_6$ ( $b_1$ ), $cm^{-1}$	83	29i	
$\nu_7$ ( $b_2$ ), $cm^{-1}$	700	743	
$\nu_8$ ( $b_2$ ), $cm^{-1}$	219	228	
$\nu_9$ ( $b_2$ ), $cm^{-1}$	150	170	

found to be 22.6 kcal/mol higher in energy at the B3LYP/6-311+G\* level of theory, similar to the  $CAI_3Si^-$  case discussed above.

**$CAI_3Ge$ .** We found two structures,  $C_{2v-I}$  ( $2B_2$ ) and  $C_{2v-II}$  ( $2B_2$ ), to be minima at the B3LYP/6-311+G\* level of theory (Figure 4 and Table 7), similar to that of  $CAI_3Si$ . Interestingly, both the  $C_{2v-I}$  and  $C_{2v-II}$  structures of  $CAI_3Ge$  were found to be perfectly planar at the MP2/6-311+G\* level of theory. We further performed calculations at the CCSD(T)/6-311+G\* level of theory and found that the  $C_{2v-I}$  structure collapsed into the  $C_{2v-II}$  structure upon geometry optimization. When geometry optimization for the  $C_{2v-II}$  structure was performed within  $C_s$  symmetry it converged to the planar structure (Table 7). We also optimized the tricoordinate  $C_{3v}$  isomer, which was found to be 8.4 kcal/mol higher in energy at the B3LYP/6-311+G\* level of theory. This result is again similar to the  $CAI_3Si$  molecule discussed above.

In summary, we obtained planar structures for all anionic and neutral species at the B3LYP/6-311+G\* level of theory. At the MP2/6-311+G\* level of theory,  $CAI_3Si^-$ ,  $CAI_3Si$ , and  $CAI_3Ge^-$  are slightly nonplanar, but after vibration averaging over the ZPE, they are actually all planar.  $CAI_3Ge$  is planar at the MP2/6-311+G\* level of theory. At our highest level of theory (CCSD(T)/6-311+G\*), only  $CAI_3Si^-$  and  $CAI_3Si$  are slightly nonplanar (planar after vibrational averaging over ZPE), while both  $CAI_3Ge^-$  and  $CAI_3Ge$  are perfectly planar.

### Interpretation of Experimental Results

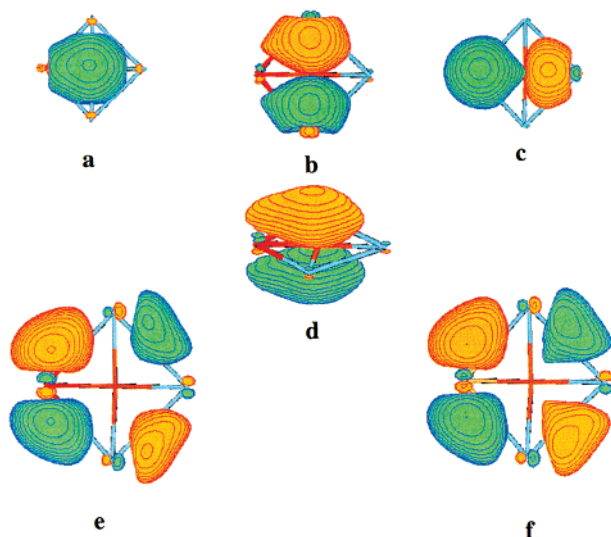
Because the deviations from planarity in  $CAI_3Si^-$ ,  $CAI_3Si$ ,  $CAI_3Ge^-$ , and  $CAI_3Ge$  are smaller than the ZPE corrections and the vibrationally averaged structures of all four species are planar, we will stick with the  $C_{2v}$  ( $1A_1$ ) planar structures in our interpretation of the experimental photoelectron spectra.

**The Tetracoordinate Planar Global Minima and the Detachment Features.** In Table 1 we present results of our calculations of the four lowest-lying vertical one-electron detachment processes from the tetracoordinate planar global minimum structures of  $CAI_3Si^-$  and  $CAI_3Ge^-$  and compare them with the experimental VDEs. The Green's function method used in this work has been shown to be able to predict VDEs within 0.2 eV. Therefore, comparison of the experimental data to the theoretical electron detachment energies provides a powerful tool to elucidate the structure and bonding of the experimentally observed species.

The positions of the calculated VDEs are also compared with the experimental spectra in Figure 2 by the vertical bars. Excellent agreement is obtained between the calculated VDEs of the tetracoordinate planar global minimal anions and the four main detachment features observed experimentally for both

**Table 7.** Calculated Molecular Properties of the  $C_{2v}$ ,  $CAI_3Ge$  Structures

	$CAI_3G(C_{2v-I}, ^2B_2)$		$CAI_3G(C_{2v-II}, ^2B_2)$		
	B3LYP/6-311+G*	MP2/6-311+G*	B3LYP/6-311+G*	MP2/6-311+G*	CCSD(T)/6-311+G*
$E_{tot}$ , au	-2842.430057	-2839.274190	-2842.431629	2839.271207	2839.336411
$\Delta E_{tot}$ , kcal/mol	0.99	0.0	0.0	1.87	---
$R(C_1-Ge_2)$ , Å	1.848	1.844	2.027	2.059	2.036
$R(C_1-Al_{3,4})$ , Å	2.036	2.046	1.997	1.999	2.003
$R(C_1-Al_3)$ , Å	2.011	2.108	1.984	1.972	1.980
$\angle Ge_2C_1Al_{3,4}$ , °	97.1	96.3	79.1	76.8	79.2
$\nu_1(a_1)$ , $cm^{-1}$	815	939	760	788	
$\nu_2(a_1)$ , $cm^{-1}$	325	334	362	389	
$\nu_3(a_1)$ , $cm^{-1}$	225	244	247	240	
$\nu_4(a_1)$ , $cm^{-1}$	166	137	205	227	
$\nu_5(b_1)$ , $cm^{-1}$	179	102	209	121	
$\nu_6(b_1)$ , $cm^{-1}$	65	54	66	42	
$\nu_7(b_2)$ , $cm^{-1}$	553	773	665	648	
$\nu_8(b_2)$ , $cm^{-1}$	236	243	242	180	
$\nu_9(b_2)$ , $cm^{-1}$	67	187	96	124	

**Figure 5.** Molecular orbital pictures.<sup>35</sup> (a–c) The three  $\sigma$ -bonding orbitals of  $CAI_3Ge^-$ , (d) the  $\pi$ -orbital of  $CAI_3Ge^-$ , (e) ligand–ligand HOMO of  $CAI_3Ge^-$ , and (f) ligand–ligand HOMO of  $CAI_3Si^-$ . The  $\sigma$ - and  $\pi$ -orbitals of  $CAI_3Si^-$  (not shown) are very similar in appearance to those for  $CAI_3Ge^-$ . Also not shown are the ligand-centered nonbonding lone-pair orbitals.

$CAI_3Si^-$  and  $CAI_3Ge^-$ . The lowest-energy peak (X), according to our calculations, involves detachment of an electron from the doubly occupied ligand–ligand bonding HOMO (labeled 3b<sub>2</sub> in Table 1, Figure 5) and produces the neutral ground state. We found that there is a slight geometry change in the neutral ground-state structures, in which the central carbon atom is distorted along the C–Si/Ge bond, resulting in a shorter C–Si bond in  $CAI_3Si$  (Table 3) and a longer C–Ge bond in  $CAI_3Ge$  (Table 7). These geometry changes between the anion ground state and the neutral ground-state result in a smaller adiabatic electron binding energies (ADE), of 2.67 eV for  $CAI_3Si^-$  and 2.66 eV for  $CAI_3Ge^-$ , compared to the 2.88 and 2.78 eV VDEs, respectively (Table 1). The relative small difference between the theoretical ADEs and VDEs, and the relative small geometry changes between the obtained structures for the anion and neutral ground states eliminate the geometry changes as a cause for the long tail of the X band, which extends to  $\sim 2$  eV (Figure 2). Although hot band transitions may still be a factor, we will show below that the tricoordinate  $C_{s,A}$  isomer possesses lower VDEs and should be the main contributor to the long tail.

Peaks A, B, and C involve detaching an electron from nonbonding ligand-centered lone-pair orbitals while leaving the

ligand–ligand bonding HOMO doubly occupied. As a result, the daughter neutrals formed in peaks A, B, and C, representing low-lying excited states of the neutral species, also retain planar geometry. The relatively narrow widths of peaks A, B, and C are consistent with electron detachment from the nonbonding ligand-centered orbitals.

#### The Low-Energy Tail and the Tricoordinate $C_{s,A}$ Isomer.

As we have shown above, the long low-energy tail in the PES spectra shown in Figure 2 cannot be accounted for by the geometry changes between the anion and neutral ground states. Although the temperatures of the anions from our source were not known, we expect them to be around room temperature, on the basis of our recent studies on pure  $Al_n^-$  clusters.<sup>32</sup> Therefore, it seems unreasonable to assume that the tail should be due to the hot band transitions. Another possibility is contributions from other isomers of the anions, which might be present in the beams.

From our extensive geometry searches, we found that the lowest-energy isomer of  $CAI_3Si^-$  above the global minimum planar structure (Figure 3a) is the tricoordinate  $C_{s,A}$  species (Figure 3b). We calculated the VDEs of this isomer and present the results in Table 8, where the experimental data and the VDEs from the planar structures are also included for comparison. The first three VDEs are also marked in Figure 2a. Two observations can be made immediately. First, we can see that the VDEs of the tricoordinate isomer are in poor agreement with the four major detachment features (X, A–C in Figure 2). Second, the ground-state VDE (2.27 eV) and ADE (2.06 eV) of the  $C_{s,A}$  isomer is much smaller than that of the planar global minimum structure. On the other hand, the 2.27 eV VDE of the  $C_{s,A}$  isomer coincides well with the low-energy tail and could be the main contributor. As shown in Figure 3, there is a large geometry change between the anion and neutral structures of the  $C_{s,A}$  isomer, suggesting the ground state detachment channel from this isomer should yield a broad band, consistent with the observation of the long tail. The abundance of this isomer should be rather small and the other higher-energy detachment channels were likely buried in the spectra of the main isomer (Figure 2a).

We tried to obtain PES spectra under different experimental conditions. However, the tail could not be eliminated completely, suggesting that there must be sizable barrier between the tricoordinate  $C_{s,A}$  isomer and the global minimum tetracoordinate structure. This is understandable upon careful examination of the two structures. One can imagine that the  $CAI_3Si^-$  cluster is

(32) Akola, J.; Manninen, M.; Hakkinen, H.; Landman, U.; Li, X.; Wang, L. S. *Phys. Rev. B* **1999**, *60*, 11297.



**Table 8.** Experimental and Theoretical Lowest VDE of Two Lowest Minima of  $\text{CaI}_3\text{Si}^-$ 

$\text{CaI}_3\text{Si}^-$ state	experimental VDE (eV)	electron detachment from MO ( $C_{2v}$ )	theoretical <sup>a</sup> VDE (eV) ( $C_{2v}$ )	electron detachment from MO ( $C_s$ )	theoretical <sup>a</sup> VDE (eV)
X	2.88(5)	$3b_2$	2.85 (0.87)	$8a'$	2.27 (0.87)
A	3.03(4)	$2b_2$	3.00 (0.87)	$7a'$	3.14 (0.86)
B	3.49(3)	$5a_1$	3.61 (0.86)	$6a'$	3.78 (0.85)
C	4.20(4)	$4a_1$	4.31 (0.84)	$1a''$	4.61 (0.85)
		$1b_1$	5.13 (0.86)	$5a'$	4.83 (0.83)

<sup>a</sup> At the OVGf/6-311+G(2df) level of theory. The pole strength is given in parentheses.

formed through nucleation of an Al atom to a planar  $\text{CaI}_2\text{Si}^-$  cluster and the two isomers are likely to result from two energetically favorable sites of nucleation of the third Al atom.

## Discussion

The photoelectron spectra, owing to vertical transitions from the anion ground state to the ground and excited states of the neutral, strongly depend on the structures of the anion and the neutral, as shown in Table 8. The excellent agreement between the theoretical and experimental results of the global minimum tetracoordinate planar structures provide solid evidence that we have indeed identified the first pentaatomic tetracoordinate planar carbon molecules in both their anion and neutral states. The previous work provided the first tetracoordinate planar carbon anion in  $\text{CaI}_4^-$ .<sup>33</sup> However, the neutral  $\text{CaI}_4$  is tetrahedral after all.

The planarity of the 18-valence-electron  $\text{CaI}_3\text{Si}^-$  and  $\text{CaI}_3\text{Ge}^-$  found here is in agreement with the prediction of previous calculations on other 18-valence-electron systems ( $\text{CaI}_2\text{Si}_2$ ,  $\text{CGa}_2\text{Si}_2$ , and  $\text{CaI}_2\text{Ge}_2$ ).<sup>13,14</sup> This planarity is expected on the basis of a straightforward valence MO occupancy model put forth in ref 14. This model begins by considering the 32-valence-electron tetrahedral  $\text{CF}_4$  molecule whose valence MO symmetries and occupancies are  $1a_1^2 1t_2^6 2a_1^2 2t_2^6 1e^4 3t_2^6 1t_1^6$ . The first four ( $1a_1^2$  and  $1t_2^6$ ) orbitals are the C–F  $\sigma$ -bonds and the remaining twelve orbitals are lone-pair orbitals localized on the F-atoms lying perpendicular ( $1e^4 3t_2^6 1t_1^6$ ) and parallel ( $2a_1^2 2t_2^6$ ) to the C–F bond axes. The above orbital occupancy clearly describes a situation with four  $\sigma$ -bonds and no net bonding or antibonding interactions among the ligands. The model assumes that the  $\text{CF}_4$  MO ordering remains valid for other tetrahedral molecules. Hence for a species with 16-valence electrons such as  $\text{CaI}_4$ , the tetrahedral structure should have a  $1a_1^2 1t_2^6 2a_1^2 2t_2^6 1e^0$  electronic configuration, which describes four  $\sigma$ -bonds ( $1a_1$  and  $1t_2$ ) and four lone-pairs ( $2a_1$  and  $2t_2$ ).<sup>14</sup> This result suggests that each Al in  $\text{CaI}_4$  can be viewed as monovalent with a 3s lone-pair. Addition of one electron to the 1e-LUMO of  $T_d$   $\text{CaI}_4$  leads to a  $1a_1^2 1t_2^6 2a_1^2 2t_2^6 1e^1$  electronic configuration for  $\text{CaI}_4^-$ , which is expected to undergo Jahn–Teller distortion toward  $D_{4h}$  ( ${}^2B_{2g}$ ). Indeed, the near-planarity of  $\text{CaI}_4^-$  is confirmed recently,<sup>33</sup> despite the fact that  $\text{CaI}_4$  neutral is tetrahedral.

These arguments suggest why 17- or 18-valence-electron species should be unstable at  $T_d$  symmetry, but why they can be stable at planar symmetry still needs to be properly explained. Insight can be obtained by examining the three  $\sigma$  ( $1a_1$ ,  $2a_1$  and  $1b_2$ ), one  $\pi$  ( $1b_1$ ), and the ligand–ligand bonding (HOMO- $3b_2$ ) orbitals, which are shown in Figure 5. The four nonbonding ligand lone-pair orbitals ( $3a_1$ ,  $4a_1$ ,  $5a_1$ , and  $2b_2$ ), whose energies lie between the ligand–ligand HOMO and the four C-ligand bonding orbitals, are not shown. The HOMOs shown in Figure

5 are clearly bonding with respect to ligand–ligand interactions and play the key role in maintaining planarity. Although the presence of one nonbonding  $\pi$ -orbital disfavors the planar geometry relative to  $T_d$ , occupation of the ligand–ligand bonding HOMO provides enough additional bonding to render the planar geometry stable and favored over  $T_d$  for 17 or 18-valence-electron pentaatomic systems.

## Concluding Remarks

It is possible that the pentaatomic planar carbon molecules observed in the gas-phase here could be synthesized in macroscopic quantity in the form of quaternary solid materials such as  $[\text{CaI}_3\text{Si}]^-\text{Na}^+$  or  $[\text{CaI}_3\text{Ge}]^-\text{Na}^+$ , which could then be characterized in further detail. The current findings suggest that a wide variety of planar, carbon-containing pentaatomic molecules with 17- or 18-valence electrons can be imagined. Several such planar molecules have already been predicted theoretically by replacing one of the ligand Al atoms in the anions treated here by Si, Ga, or Ge.<sup>13,14</sup> The central C can also be replaced to obtain more planar molecules; for example,  $\text{Al}_4\text{N}$  and  $\text{Al}_4\text{N}^-$ ,  $\text{Al}_3\text{SiN}$  and  $\text{Si}_3\text{AlB}$ , which have been studied previously, are all planar.<sup>13,34</sup> Planar molecules involving other central atoms, such as Si, P, or Ge, are likely to exist and would be extremely interesting to investigate. Planarity in  $\text{CaI}_3\text{Si}$ ,  $\text{CaI}_3\text{Ge}$ ,  $\text{CaI}_3\text{Si}^-$ , and  $\text{CaI}_3\text{Ge}^-$  is achieved through ligand–ligand bonding interactions and occupation (singly or doubly) of the ligand–ligand bonding HOMO. While the central cavity in  $\text{CaI}_3\text{Si}$  and  $\text{CaI}_3\text{Si}^-$  is slightly too small to accommodate the carbon atom in a perfectly planar environment, vibrational averaging results in a planar structure. On the other hand, perfect planarity is indeed achieved at the potential energy surface minimum in  $\text{CaI}_3\text{Ge}$  and  $\text{CaI}_3\text{Ge}^-$ .

**Acknowledgment.** The theoretical work was done at the University of Utah and at Utah State University. The work at the University of Utah is supported by the National Science Foundation (CHE-9618904) and the work at Utah State University is supported by donors of the Petroleum Research Fund (ACS-PRF# 35255-AC6), administered by the American Chemical Society. We acknowledge the Center for High Performance Computations at the University of Utah for computer time. The experimental work done at Washington is supported by the National Science Foundation (DMR-9622733). The experiment was performed at the W. R. Wiley Environmental Molecular Sciences Laboratory, a national scientific user facility sponsored by DOE's Office of Biological and Environmental Research and located at Pacific Northwest National Laboratory, which is operated for DOE by Battelle under Contract DE-AC06-76RLO 1830. L.S.W. is an Alfred P. Sloan Foundation Research Fellow.

JA993081B

(34) Nayak, S. K.; Rao, B. K.; Jena, P.; Li, X.; Wang, L. S. *Chem. Phys. Lett.* **1999**, *301*, 379.

(35) The MO pictures were made using the MOLDEN3.4 program. Schaftenaar, G. *MOLDEN3.4*, CAOS/CAMM Center; The Netherlands 1998.

(33) Li, X.; Wang, L. S.; Boldyrev, A. I.; Simons, J. *J. Am. Chem. Soc.* **1999**, *121*, 6033.